

Simulated diffusion dataset for multi-tensor fiber tractography

Arish A. Qazi^{1,2}, Gordon Kindlmann², Carl-Fredrik Westin²

¹University of Copenhagen, Denmark, ²Department of Radiology, Harvard Medical School, USA

Introduction

An inherent drawback of the traditional diffusion tensor model is the inability to capture more than one fiber orientation within a voxel. This leads to erroneous results in fiber tractography specifically in locations where fiber bundles cross each other. Thus, there is a shift towards quantifying the complex fiber architecture by more sophisticated models of diffusion, such as the partial volume model (1). The traditional tractography technique, however, is unable to incorporate these complex models and as a result new deterministic and probabilistic tractography methods are emerging (2). The verification of the resultant trace-lines from these methods, however, is difficult; since there is no other method that can determine the real trajectory in-vivo. Thus in the absence of a gold standard it is extremely difficult to validate and compare the different tractography techniques. In this paper, we present a simulated diffusion weighted dataset, generated with parameters similar to an MR sequence, and designed specifically for validating a two-tensor based tractography method.

Methods

Two anisotropic tensors with eigenvalues 1.7, 0.2, $0.2 \times 10^{-3} \text{ mm}^2/\text{s}$ were simulated, corresponding to the eigenvalues in the splenium of the corpus callosum (3). The underlying diffusion was modeled as a simple mixture of Gaussian densities, represented by the following equation

$$S = S_0 \left(f e^{-b g^t D_1 g} + (1 - f) e^{-b g^t D_2 g} \right)$$

Where D_1 and D_2 are the two tensors. For each slice of the dataset a crossing region was defined by varying the angle between the principal eigenvectors of the two tensors in 2° steps from $0 - 90^\circ$, yielding 45 slices. Outside the crossing region there was only one anisotropic tensor, and at the borders the tensor was isotropic. The diffusion equation was then used to estimate the DWI's for each voxel of the image. The fraction of signal for the two anisotropic tensors in the crossing region was kept at 0.5. The dataset was generated with 55 gradient directions, $b = 1000 \text{ s}/\text{mm}^2$, and 5 non-diffusion-weighted images. Additionally the image was smoothed and complex Gaussian noise was added to simulate an SNR of 18, 20, and 22. The dataset was tested by reconstructing the trace-lines by means of the traditional single (4) and our two-tensor tractography method (5). The dataset can be downloaded from www.diku.dk/~arish/software.

Results

Fig. 1 illustrates a slice showing a simulated 60° crossing. Fig.2 shows a slice with addition of Gaussian noise, and illustrates the trace-lines from the single and two-tensor tractography. The figures shows that for the single tensor case one expects the fibers to continue horizontally, instead as they approach the crossing region the fiber tracts diverge laterally, in the wrong direction. In contrast two-tensor tractography is able to depict the correct behavior, by running straight through the overlapping region.



Figure. 1. The simulated 60° fiber crossing. Inside the brown region (middle), two anisotropic tensors are crossing each other. Outside the region there is one anisotropic tensor, and the direction is color-coded.

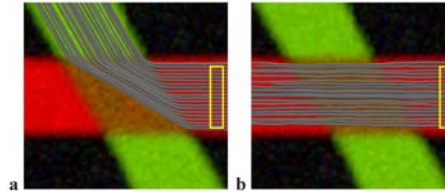


Figure. 2. Simulated 60° fiber crossing with the addition of Gaussian noise at an SNR of 18. Trace-lines from (when seeded in the region bounded by the yellow box): (a) Single tensor tractography. (b) Two-tensor tractography.

Discussion

We have designed a synthetic dataset that allows validation and comparison of two-tensor based tractography techniques. The dataset will allow for quantitative evaluations of the different two-tensor based tractography methods (in varying noise conditions), in contrast to the current qualitative evaluation by visual inspection. Future work will involve extending the dataset to higher models of diffusion.

References: **1.** Blyth et al., ISMRM 2003; **2.** Parker., ISMRM 2006; **3.** Pierpaoli et al., Radiology 201:637-648, 1996; **4.** Basser et al., MRM 44:625-632, 2000; **5.** Qazi et al., MRM (Submitted).